

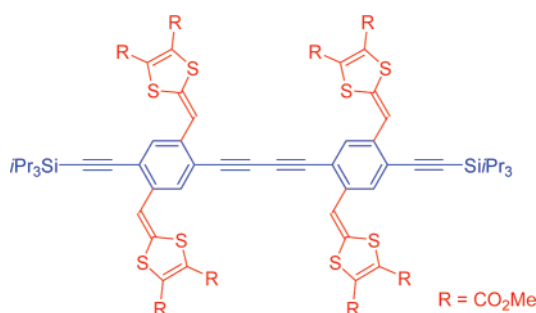
Synthesis and Characterization of Cruciform-Conjugated Molecules Based on Tetrathiafulvalene

Mikkel Vestergaard, Karsten Jennum, Jakob Kryger Sørensen, Kristine Kilså, and Mogens Brøndsted Nielsen*

Department of Chemistry, University of Copenhagen, Universitetsparken 5, DK-2100 Copenhagen Ø, Denmark

mbn@kiku.dk

Received January 2, 2008



Stepwise acetylenic scaffolding provides cruciform-conjugated molecules with vertically disposed π -systems, one being an extended tetrathiafulvene (TTF) unit. Two synthetic routes for a cruciform dimer incorporating a total of two extended TTFs was developed, employing either an oxidative Hay coupling reaction as the final dimerization step or as one of the initial steps. Both routes take advantage of ready access to new mono- and diethynylbenzene building blocks incorporating a variety of other functionalities. The redox and optical properties of the cruciform molecules were investigated by cyclic and differential pulse voltammetries and UV–vis absorption spectroscopy. The access to multiple redox states renders the molecules attractive candidates as wires, or possibly transistors, for molecular electronics. Generation of a quinoid structure by oxidation is supported by density functional theory calculations.

Introduction

Cruciform molecules containing two perpendicularly disposed π -systems are attractive as molecular wires and switches for molecular electronics and advanced materials¹ because of their multiple linear and cross-conjugated pathways for electron delocalization. Recent examples of cruciform-conjugated molecules include bis-phenyloxazole/terphenyl systems,² several oligo(phenylenevinylene) and oligo(phenyleneethynylene) structures,³ functionalized tetraethynylethenes,⁴ and acetylenic scaffolds of 9,10-bis(1,3-dithiol-2-ylidene)-9,10-dihydroanthracene.⁵ We recently devised an efficient synthesis of the cruciform molecule **1** incorporating the redox-active tetrathiafulvalene

(TTF) donor together with an oligo(phenyleneethynylene) OPE3 backbone.⁶ TTF exhibits two reversible one-electron oxidation steps and has for this reason found wide applications in both materials and supramolecular chemistry.⁷ The conjugation

(1) (a) Gholami, M.; Tykwinski, R. R. *Chem. Rev.* **2006**, *106*, 4997–5027. (b) Galbrecht, F.; Bünnagel, T. W.; Bilge, A.; Scherf, U.; Farrell, T. In *Functional Organic Molecules*; Müller, T. J. J., Bunz, U. H. F., Eds.; Wiley-VCH: Weinheim, 2007; pp 83–118. (c) Weibel, N.; Grunder, S.; Mayor, M. *Org. Biomol. Chem.* **2007**, *5*, 2343–2353.

(2) Klare, J. E.; Tulevski, G. S.; Sugo, K.; de Picciotto, A.; White, K. A.; Nuckolls, C. *J. Am. Chem. Soc.* **2003**, *125*, 6030–6031.

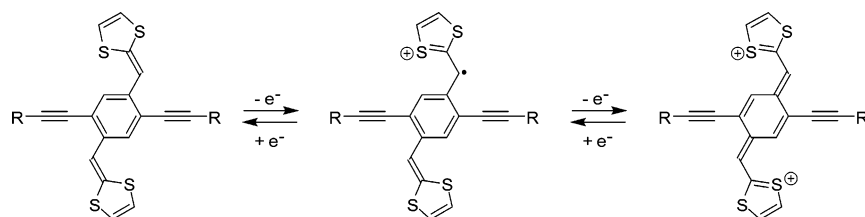
(3) (a) Wilson, J. N.; Josowicz, M.; Wang, Y.; Bunz, U. H. F. *Chem. Commun.* **2003**, 2962–2963. (b) Wilson, J. N.; Bunz, U. H. F. *J. Am. Chem. Soc.* **2005**, *127*, 4124–4125. (c) Marsden, J. A.; Miller, J. J.; Shirliff, L. D.; Haley, M. M. *J. Am. Chem. Soc.* **2005**, *127*, 2464–2476. (d) Spitler, E. R.; Shirliff, L. D.; Haley, M. M. *J. Org. Chem.* **2007**, *72*, 86–96. (e) McGrier, P. L.; Solntsev, K. M.; Schönhaber, J.; Brombosz, S. M.; Tolbert, L. M.; Bunz, U. H. F. *Chem. Commun.* **2007**, 2127–2129. (f) Gerhardt, W. W.; Zuccherro, A. J.; South, C. R.; Bunz, U. H. F.; Weck, M. *Chem.—Eur. J.* **2007**, *13*, 4467–4474. (g) Grunder, S.; Huber, R.; Horhoiu, González, M. T.; Schönenberger, C.; Calame, M.; Mayor, M. *J. Org. Chem.* **2007**, *72*, 8337–8344. (h) Zhou, N.; Wang, L.; Thompson, D. W.; Zhao, Y. *Tetrahedron Lett.* **2007**, *48*, 3563–3567. (i) Błaszczak, A.; Fischer, M.; von Hänisch, C.; Mayor, M. *Eur. J. Org. Chem.* **2007**, 2630–2642.

(4) (a) Tykwinski, R. R.; Schreiber, M.; Carlón, R. P.; Diederich, F.; Gramlich, V. *Helv. Chim. Acta* **1996**, *79*, 2249–2280. (b) Nielsen, M. B.; Diederich, F. *Chem. Rev.* **2005**, *105*, 1837–1867.

(5) Chen, G.; Zhao, Y. *Tetrahedron Lett.* **2006**, *47*, 5069–5073.

(6) Sørensen, J. K.; Vestergaard, M.; Kadziola, A.; Kilså, K.; Nielsen, M. B. *Org. Lett.* **2006**, *8*, 1173–1176.

SCHEME 1. Generation of Quinoid Structure upon Two-Electron Oxidation

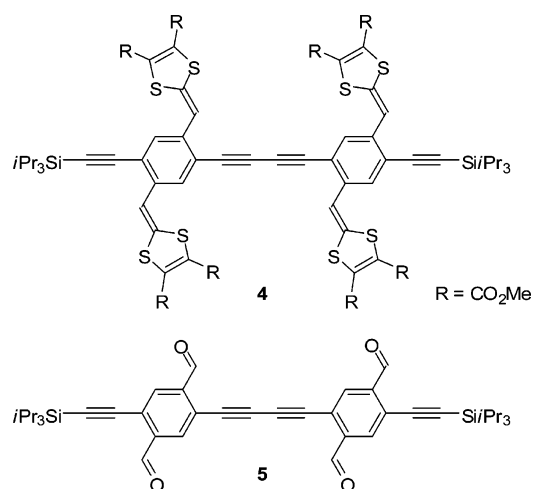
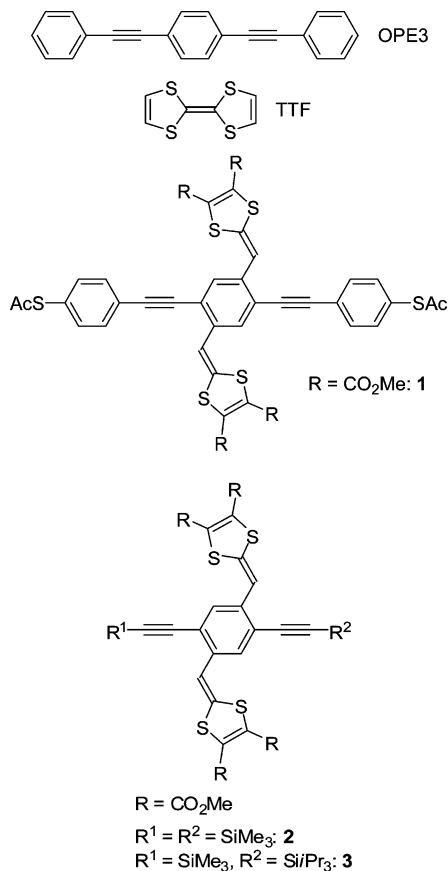


pathway along the OPE moiety of **1** is expected to change from linearly to cross-conjugated upon oxidation of the vertically appended TTF as the dication should take a quinoid structure at the central benzene ring (Scheme 1). This change in conjugation pathway along the OPE is assumed to be accompanied by a change in the conductivity (on/off). We imagine that this switching could be accomplished by tuning a gate potential in a three-electrode field-effect transistor in which the two thiol end-groups of the OPE unit is connected to source and drain electrodes made of gold. Hummelen and co-workers⁸ recently employed the same underlying principle of “conjugation pathway switching” in the design of an anthraquinone redox-controlled wire. Indeed, numerous reports have revealed the inefficiency of cross conjugation for electron delocalization in acyclic molecules, for example, in dendralenes,⁹ expanded dendralenes,¹⁰ and dithiafulvene oligomers.¹¹ In a synthesis-driven approach, we aim at developing efficient synthetic protocols for oligomeric TTF-based, redox-active cruciforms. It should be mentioned that other interesting combinations of TTF and OPE (or derivatives thereof) in which the TTF unit is part of the lateral backbone have been reported.¹²

The previously reported⁶ synthesis of compound **1** was achieved from the diacetylenic building block **2** containing two

identical trimethylsilyl protected terminal acetylenes. Here, we report an efficient route to the unsymmetrical compound **3** containing two different trialkylsilyl end-groups to allow for stepwise desilylation and hence stepwise acetylenic scaffolding. We have employed this compound for the synthesis of the cruciform dimer **4**. Alternatively, this dimer can be prepared by a four-fold Wittig reaction of the tetraaldehyde **5**. The synthetic routes to both compounds **3** and **4** provide a selection of intermediate building blocks that are useful for acetylenic scaffolding in general. It is also noteworthy that we have previously in our work on acetylenic TTF scaffolding experienced considerable instability of the intermediate terminal acetylenes.¹³ This instability has to a large extent been overcome in the modules **2** and **3**. In addition to synthetic protocols, the optical and electrochemical properties of the new cruciform molecules are presented. We have also subjected the dication formed upon oxidation to a computational study to elucidate the degree of quinoid character and hence the rationale behind the design.

We shall briefly mention that examples of molecules incorporating a total of four dithiafulvene units about a central conjugated core, such as compound **4**, are rather limited in the literature and include structures based on anthraquinone cores,¹⁴ a [4]radialene core,¹⁵ or a single benzene core.¹⁶ OPEs functionalized with redox-active fullerenes have been reported,¹⁷ but here the fullerenes are isolated from the OPE via nonconjugated linkers.

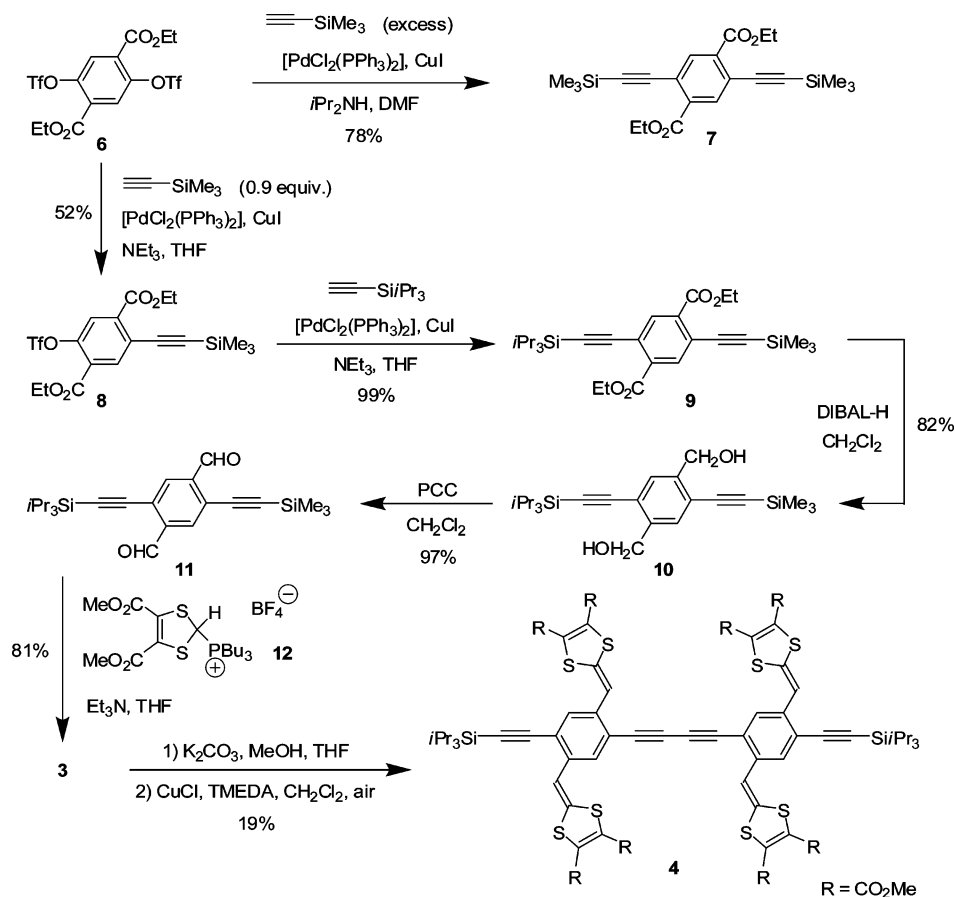


(7) (a) Bryce, M. R. *Adv. Mater.* **1999**, *11*, 11–23. (b) Nielsen, M. B.; Lomholt, C.; Becher, J. *Chem. Soc. Rev.* **2000**, *29*, 153–164. (c) Bryce, M. R. *J. Mater. Chem.* **2000**, *10*, 589–598. (d) Segura, J. L.; Martín, N. *Angew. Chem., Int. Ed.* **2001**, *40*, 1372–1409.

(8) van Dijk, E. H.; Myles, D. J. T.; van der Veen, M. H.; Hummelen, J. C. *Org. Lett.* **2006**, *8*, 2333–2336.

(9) (a) Brain, P. T.; Smart, B. A.; Robertson, H. E.; Davis, M. J.; Rankin, D. W. H.; Henry, W. J.; Gosney, I. *J. Org. Chem.* **1997**, *62*, 2767–2773. (b) Fielder, S.; Rowan, D. D.; Sherburn, M. S. *Angew. Chem., Int. Ed.* **2000**, *39*, 4331–4333.

SCHEME 2



Results and Discussion

Our synthesis starts from the readily available ditriflate **6**¹⁸ (Scheme 2). Treatment of this compound with an excess of trimethylsilylacetylene under Sonogashira cross-coupling conditions¹⁹ furnished the diacetylenic product **7**.⁶ Using slightly less than one equivalent of the acetylene provided conveniently the

monoalkynylated product **8** in a fair yield of 52% after careful column chromatographic workup. Next, a second cross-coupling reaction with triisopropylsilylacetylene gave the differentially protected diacetylenic product **9** in quantitative yield. The ethyl ester groups were reduced with diisobutylaluminum hydride (DIBAL-H) to provide the diol **10**. This compound was then oxidized by pyridinium chlorochromate (PCC) affording the dialdehyde **11**. A two-fold Wittig reaction with the phosphonium salt **12** and triethylamine as base gave the extended TTF **3**. A selective desilylation of the SiMe_3 group by K_2CO_3 in MeOH/THF followed by an oxidative Hay coupling reaction²⁰ gave the dimer target **4**, albeit in modest yield.

The second route to the dimer **4** starts with a Hay dimerization reaction as presented in Scheme 3. First, compound **9** was selectively desilylated to the terminal acetylene **13**. Under these reactions conditions, the ethyl ester groups were transesterified to methyl ester groups. Compound **13** was then oxidatively homocoupled to form the butadiyne product **14** that was subsequently treated with DIBAL-H to furnish the tetraol **15**. A four-fold oxidation using PCC gave the tetraaldehyde **5**. A final four-fold Wittig reaction with the phosphonium salt **12** and triethylamine ultimately gave the dimer **4**.

Compound **8** also served as a precursor for other useful acetylenic building blocks as shown in Scheme 4. Reduction with DIBAL-H gave the diol **16** that was then oxidized to the dialdehyde **17**. Two-fold Wittig reaction subsequently gave the extended TTF **18** incorporating both a reactive triflate group and a protected terminal acetylene group.

(10) Burri, E.; Diederich, F.; Nielsen, M. B. *Helv. Chim. Acta* **2002**, *85*, 2169–2182.

(11) Nielsen, M. B.; Petersen, J. C.; Thorup, N.; Jessing, M.; Andersson, A. S.; Jepsen, A. S.; Gisselbrecht, J.-P.; Boudon, C.; Gross, M. *J. Mater. Chem.* **2005**, *15*, 2599–2605.

(12) (a) Wang, C.; Batsanov, A. S.; Bryce, M. R. *Chem. Commun.* **2004**, 578–579. (b) Wang, E.; Li, H.; Hu, W.; Zhu, D. *J. Polym. Science, Part A: Polymer Chem.* **2006**, *44*, 2707–2713.

(13) (a) Nielsen, M. B.; Utesch, N. F.; Moonen, N. N. P.; Boudon, C.; Gisselbrecht, J.-P.; Concilio, S.; Piotto, S. P.; Seiler, P.; Günter, P.; Gross, M.; Diederich, F. *Chem.—Eur. J.* **2002**, *8*, 3601–3613. (b) Nielsen, M. B. *Synlett* **2003**, 1423–1426.

(14) (a) Martín, N.; Pérez, I.; Sánchez, L.; Seoane, C. *J. Org. Chem.* **1997**, *62*, 870–877. (b) Díaz, M. C.; Illescas, B. M.; Seoane, C.; Martín, N. *J. Org. Chem.* **2004**, *69*, 4492–4499. (c) Díaz, M. C.; Illescas, B. M.; Martín, N.; Perepichka, I. F.; Bryce, M. R.; Levillain, E.; Viruela, R.; Ortí, E.; *Chem.—Eur. J.* **2006**, *12*, 2709–2721. (d) Ryhding, T.; Petersen, M. Å.; Kilså, K.; Nielsen, M. B. *Synlett* **2007**, *6*, 913–916.

(15) Misaki, Y.; Matsumura, Y.; Sugamoto, T.; Yoshida, Z. *Tetrahedron Lett.* **1989**, *30*, 5289–5292.

(16) Salle, M.; Belyasmine, A.; Gorgues, A.; Jubault, M.; Soyer, N. *Tetrahedron Lett.* **1991**, *32*, 2897–2900.

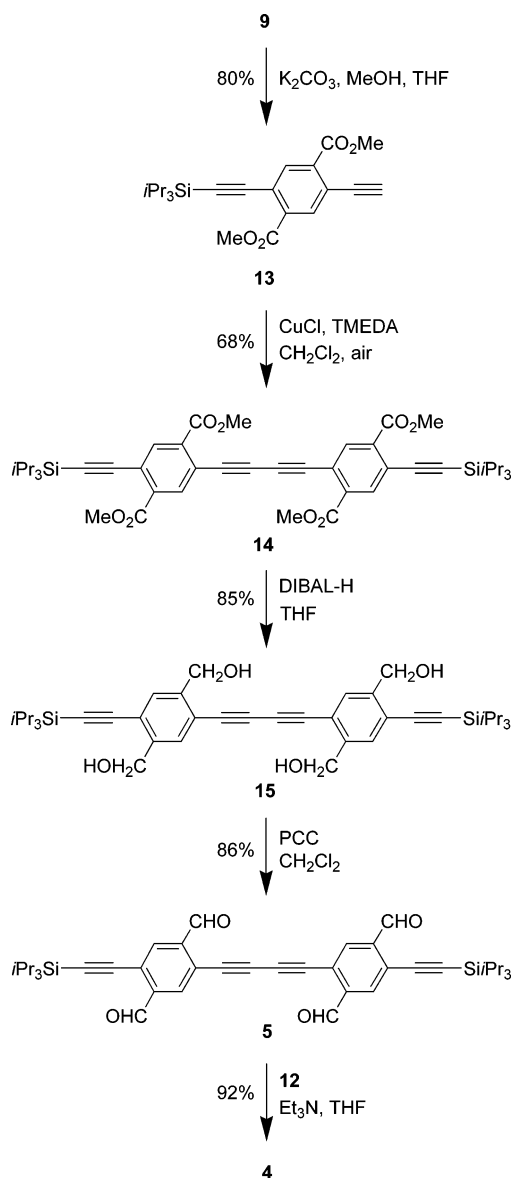
(17) de la Cruz, J. L. D.; Hahn, U.; Nierengarten, J.-F. *Tetrahedron Lett.* **2006**, *47*, 3715–3718.

(18) Zhang, Q.; Shi, C.; Zhang, H.-R.; Wang, K. K. *J. Org. Chem.* **2000**, *65*, 7977–7983.

(19) Sonogashira, K.; Tohda, Y.; Hagihara, N. *Tetrahedron Lett.* **1975**, 4467–4470.

(20) Hay, A. S. *J. Org. Chem.* **1962**, *27*, 3320–3321.

SCHEME 3



Electrochemistry. The redox properties of the cruciform TTFs were studied by cyclic voltammetry (CV) and differential pulse voltammetry (DPV). The data are collected in Table 1 and voltammograms are shown in Figure 1. According to CV, compound **3** exhibits three separated and quasireversible oxidations. The first two oxidations of **3** are interpreted as one-electron oxidations originating from oxidation of each dithiaful-

fulvene ring (Scheme 1). The third oxidation is presumably oxidation of the central backbone. A nonaromatic quinoid structure of the dication may facilitate this oxidation of the backbone (vide supra).

Cyclic voltammetry of the dimer **4** revealed two broad waves. However, DPV revealed a shoulder to the first oxidation step (inset in Figure 1). Somewhat surprisingly, the oxidations of **4** are anodically shifted relative to those of the monomer **3** although the charge can be delocalized over a larger conjugated area. A similar decrease in donor strength has nevertheless been observed for other large acetylenic scaffolds of TTF.²¹

Absorption Spectroscopy. The absorption spectra of very dilute solutions of compounds **3** and **4** in CHCl_3 are revealed in Figure 2. The monomer **3** exhibits absorption maxima at λ_{max} 311, 405, and 422 nm with molar absorptivities (ϵ) of 42 300, 38 000, and 37 900 $\text{M}^{-1}\text{cm}^{-1}$, respectively. The dimer **4** is a very strong chromophore basically in the entire region from ca. 300 to 500 nm with broad absorption maxima: λ_{max} (ϵ) = 331 nm (66 000 $\text{M}^{-1}\text{cm}^{-1}$), 386 nm (72 600 $\text{M}^{-1}\text{cm}^{-1}$), 437 (shoulder) nm. Accordingly, the low-energy absorption of **4** is red-shifted relative to that of **3**, which is explained by the extended conjugation in **4**.

Computational Study. To investigate further the possibility of forming a quinoid character upon removing two electrons from **3**, we subjected the related compound **19** (Figure 3) devoid of the CO_2Me substituents to a computational study using the Gaussian 03 program package.²² First, geometry-optimizations were performed at the B3LYP/6-31G(d) level for both the neutral and dication structures. A frequency analysis was performed in each case to ascertain that a real minimum had been obtained (i.e., no imaginary vibrational frequencies). The obtained structure of the neutral compound has each dithiaful-

(21) Andersson, A. S.; Qvortrup, K.; Torbensen, E. R.; Mayer, J.-P.; Gisselbrecht, J.-P.; Boudon, C.; Gross, M. Kadziola, A.; Kilså, K.; Nielsen, M. B., *Eur. J. Org. Chem.* **2005**, 3660–3671.

(22) Frisch, M. J.; Trucks, G. W.; Schlegel, H. B.; Scuseria, G. E.; Robb, M. A.; Cheeseman, J. R.; Montgomery, J. A., Jr.; Vreven, T.; Kudin, K. N.; Burant, J. C.; Millam, J. M.; Iyengar, S. S.; Tomasi, J.; Barone, V.; Mennucci, B.; Cossi, M.; Scalmani, G.; Rega, N.; Petersson, G. A.; Nakatsuji, H.; Hada, M.; Ehara, M.; Toyota, K.; Fukuda, R.; Hasegawa, J.; Ishida, M.; Nakajima, T.; Honda, Y.; Kitao, O.; Nakai, H.; Klene, M.; Li, X.; Knox, J. E.; Hratchian, H. P.; Cross, J. B.; Adamo, C.; Jaramillo, J.; Gomperts, R.; Stratmann, R. E.; Yazyev, O.; Austin, A. J.; Cammi, R.; Pomelli, C.; Ochterski, J. W.; Ayala, P. Y.; Morokuma, K.; Voth, G. A.; Salvador, P.; Dannenberg, J. J.; Zakrzewski, V. G.; Dapprich, S.; Daniels, A. D.; Strain, M. C.; Farkas, O.; Malick, D. K.; Rabuck, A. D.; Raghavachari, K.; Foresman, J. B.; Ortiz, J. V.; Cui, Q.; Baboul, A. G.; Clifford, S.; Cioslowski, J.; Stefanov, B. B.; Liu, G.; Liashenko, A.; Piskorz, P.; Komaromi, I.; Martin, R. L.; Fox, D. J.; Keith, T.; Al-Laham, M. A.; Peng, C. Y.; Nanayakkara, A.; Challacombe, M.; Gill, P. M. W.; Johnson, B.; Chen, W.; Wong, M. W.; Gonzalez, C.; Pople, J. A. *Gaussian 03*, revision B.03; Gaussian, Inc.: Pittsburgh, PA, 2003.

SCHEME 4

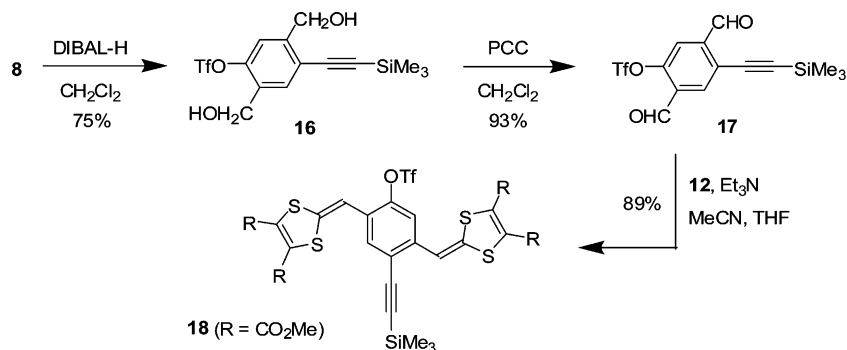


TABLE 1. Potentials^a Obtained from Cyclic Voltammetry (CV) and Differential Pulse Voltammetry (DPV) Data

compound	CV ^b			DPV		
	E_{ox}^1 (E_{pa}^1 ; E_{pc}^1) V vs Fc ^{+/0} /Fc	E_{ox}^2 (E_{pa}^2 ; E_{pc}^2) V vs Fc ^{+/0} /Fc	E_{ox}^3 (E_{pa}^3 ; E_{pc}^3) V vs Fc ^{+/0} /Fc	E_{ox}^1 V vs Fc ^{+/0} /Fc	E_{ox}^2 V vs Fc ^{+/0} /Fc	E_{ox}^3 V vs Fc ^{+/0} /Fc
3	0.56 (0.61; 0.51)	0.67 (0.70; 0.64)	0.93 (0.98; 0.88)	0.52	0.63	0.90
4	0.61 (br) (0.66; 0.56)	0.96 (br) (1.03; 0.89)		0.53	0.63 (sh)	0.91

^a All the potentials were determined in CH₂Cl₂ using Ag/Ag⁺ as a reference electrode, Pt as the counter electrode, and glassy carbon as the working electrode. Supporting electrolyte: 0.1M NBu₄PF₆. ^b E_{ox} is the half-wave potential; E_{pa} and E_{pc} are the anodic and cathodic peak potentials. Scan rate 100 mV s⁻¹.

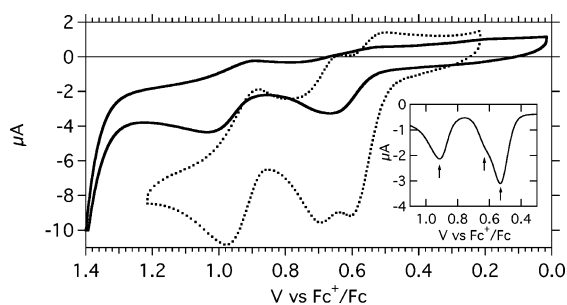


FIGURE 1. CV of **3** (dotted line) and **4** (solid line) in CH₂Cl₂ with 0.1 M Bu₄NPF₆. Inset shows DPV of **4** with arrows marking the three oxidation peaks.

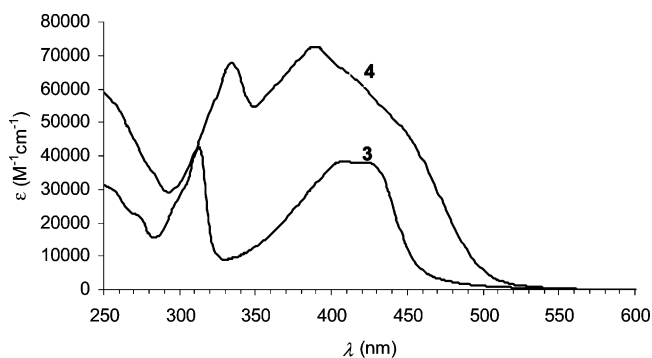


FIGURE 2. Absorption spectra of **3** (2.8×10^{-5} M) and **4** (1.5×10^{-5} M) in CHCl₃.

vene ring rotated by an angle of 15° relative to the plane defined by the central benzene ring, while the three rings are maintained in the same plane in the structure of the dication (deviation of only 0.07°). From the bond lengths, the quinoid characters along the backbone of the molecule ($\delta r_{||}$) and vertically to the backbone (δr_{\perp} , Figure 3) were calculated. The quinoid character vertically to the wire increases significantly from 0.017 in the neutral compound to 0.074 in the dication. In accordance hereto, the length of the fulvene C–C bond (a) increases from 1.357 to 1.418 Å. The quinoid character along the wire decreases upon oxidation. Only minor changes are observed for the C–C≡C bond (f, g) lengths. The quinoid structure of **19**²⁺ with a cross-conjugated pathway along the wire supports the idea as stated above of exploring these molecules as transistors for molecular electronics.

The electrochemical experiments reveal that compound **3** undergoes a third oxidation step, which we ascribe to oxidation of the central backbone. Disruption of the aromatic backbone by the formation of a quinoid structure may facilitate this third oxidation. Thus, we find by DFT calculations (B3LYP/6-311++G(2d,p)) that the vertical ionization energies of the model compounds **20** and **21** (Figure 4) are 7.94 and 7.58 eV,

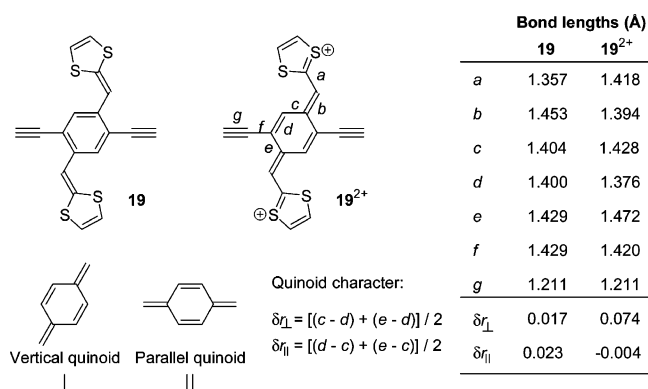


FIGURE 3. Bond lengths obtained by geometry-optimization (B3LYP/6-31G(d)) and quinoid characters along the vertical and parallel directions of the neutral and dicationic compounds.

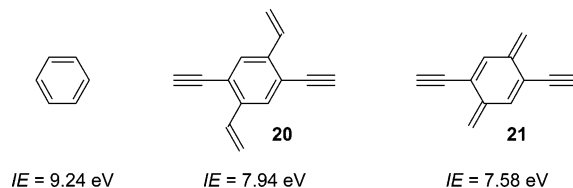


FIGURE 4. Calculated vertical ionization energies (B3LYP/6-311++G(2d,p)).

respectively, and that of benzene is 9.28 eV, which is in good agreement with an experimental value²³ of 9.24 eV. It transpires that the quinoid compound **21**, resembling the central part of **3**²⁺, has a significantly smaller ionization energy than that of compound **20** containing an intact benzene ring. Both compounds are much stronger electron donors than benzene.

A dimer structure (**22**) devoid of both the ester and triisopropylsilyl substituents was also geometry-optimized at the B3LYP/6-31G(d) level (Figure 5). Again the two dithiafulvene rings are slightly distorted from the plane defined by each benzene ring (13–14°). In addition, the two units are rotated relative to each other; thus, the two benzene rings are rotated by ca. 30° relative to each other. The frontier orbitals of both **19** and **22** are shown in Figure 6. The highest occupied molecular orbital (HOMO) of the dimer is mainly located at the two extended TTF units, while the lowest unoccupied molecular orbital (LUMO) is mainly located at the central phenyleneethynylene backbone. This orthogonal orientation of the HOMO and LUMO relative to each other supports the idea behind the cruciform design. Electron transport in a field-effect transistor can occur through a LUMO, which is favorably

(23) Nemeth, G. I.; Selzle, H. L.; Schlag, E. W. *Chem. Phys. Lett.* **1993**, *215*, 151–155 and references cited therein.

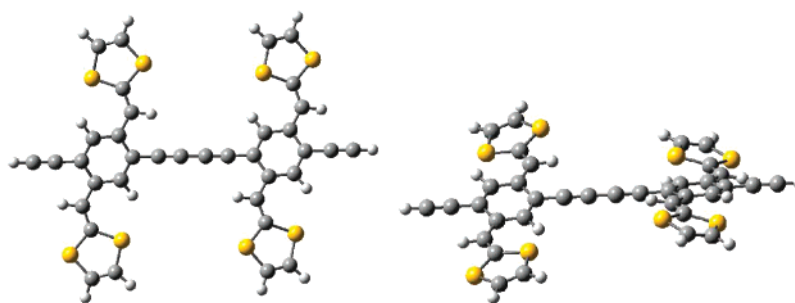


FIGURE 5. Optimized structure of dimer **22** (B3LYP/6-31G(d)).

aligned along the wire in the neutral molecule. Upon two-electron oxidation, the depicted HOMO becomes the new orthogonally disposed LUMO, now unfavorably aligned.

Conclusions

Cruciform-conjugated molecules based on extended TTFs were prepared from a variety of acetylenic precursors. In particular, the synthetic protocols benefit from ready access to aromatic building blocks containing both triflate and ethynyl functional groups allowing for stepwise acetylenic scaffolding via metal-catalyzed cross-coupling reactions. The cruciform TTFs are stable and undergo quasireversible oxidations, which makes the structural motifs interesting as potential wires for molecular electronics. According to a computational study, generation of a quinoid structure upon oxidation seems likely and substantiates the design behind these molecules. The potential strength of the cruciform design for molecular electronics applications also manifests itself in the orthogonally disposed HOMO and LUMO.

Previously, it was shown⁶ that end-capping with thiol groups to allow for adhesion of the molecules between gold electrodes is readily performed. Yet, the sulfurs present in the dithiafulvenes may on the other hand complicate a proper orientation of the cruciforms between gold electrodes. Substitution of the methoxycarbonyl ester substituents by more bulky groups, hereby rendering the heterocyclic sulfur atoms inaccessible, may solve this problem in the further refinement of these first prototype molecules.

Experimental Section

Compound 8. Diethyl-2,5-bis(trifluoromethylsulfonyloxy)-terephthalate **6** (5.00 g, 9.65 mmol), Pd(PPh₃)₂Cl₂ (0.20 g, 0.29 mmol), and CuI (0.10 g, 0.53 mmol) were dissolved in dry, argon-degassed THF (25 mL). Then argon-degassed NEt₃ (10 mL) and trimethylsilylacetylene (1.13 mL, 8.20 mmol) were added. After stirring for 24 h at rt, the reaction mixture was poured into CH₂Cl₂ (250 mL) and washed with saturated aqueous ammonium chloride (2 × 150 mL) and brine (100 mL). The organic phase was dried (MgSO₄), filtered, and evaporated to dryness under reduced pressure to give a red-brown semisolid. Column chromatography (SiO₂, EtOAc/heptane 1:9) gave the product **8** as an oil, which slowly solidified upon standing (1.990 g, 52%). ¹H NMR (300 MHz, CDCl₃): δ = 0.28 (s, 9H), 1.40–1.55 (m, 6H), 4.40–4.50 (m, 4H), 7.79 (s, 1H), 8.23 (s, 1H). ¹³C NMR (75 MHz, CDCl₃): δ = −0.2, 14.2, 14.2, 62.4, 62.9, 100.7, 103.9, 112.4/116.7/120.9/125.2 (−CF₃), 123.9, 124.8, 127.5, 137.4, 138.9, 146.7, 162.7, 164.1. MS (FAB) *m/z*: 467.1

= [M + H⁺]. Anal. Calcd for C₁₈H₂₁O₇SSi: C, 46.34; H, 4.54. Found: C, 46.52; H, 4.47.

Compound 9. The triflate **8** (1.00 g, 2.14 mmol), Pd(PPh₃)Cl₂ (0.045 g, 0.06 mmol), and CuI (0.025 g, 0.13 mmol) were dissolved in dry, argon-degassed THF (30 mL). Then degassed NEt₃ (10 mL) and triisopropylsilylacetylene (0.096 mL, 4.292 mmol) were added, and the reaction mixture was stirred for 48 h at rt. Then the reaction mixture was poured into CH₂Cl₂ (250 mL) and washed with saturated aqueous NH₄Cl (2 × 150 mL). The organic phase was dried (MgSO₄), filtered, and evaporated to dryness under reduced pressure to give a brown oil. Column chromatography (SiO₂, EtOAc/heptane 1:4) gave the product **9** (1.053 g, 99%) as a clear oil. ¹H NMR (300 MHz, CDCl₃): δ = 0.27 (s, 9H), 1.11–1.14 (m, 21H), 1.36–1.44 (m, 6H), 4.36–4.45 (m, 4H), 8.00 (s, 1H), 8.03 (s, 1H). ¹³C NMR (75 MHz, CDCl₃): δ = −0.1, 11.4, 14.4 (×2; i.e., two signals), 18.8, 61.9 (×2), 99.9, 102.3, 102.5, 103.9, 122.5, 123.0, 134.9, 135.4, 136.1, 136.5, 165.3, 165.5. MS (FAB): *m/z* = 499.3 [M + H⁺]. Anal. Calcd for C₂₈H₄₂O₄Si₂: C, 67.42; H, 8.49. Found: C, 67.50; H, 8.67.

Compound 10. The diester **9** (1.04 g, 2.08 mmol) was dissolved in dry CH₂Cl₂ (9 mL), and the mixture was cooled to 0 °C. Then DIBAL-H (16.7 mL, 16.7 mmol, 1M in hexane) was added during 10 min. After stirring for 3.5 h at 0 °C, the mixture was poured into aqueous NH₄Cl (110 mL). Then CH₂Cl₂ (110 mL) was added, and the mixture was stirred for 10 min. The resulting gel was passed through a short column of Celite. The layer was washed with CH₂Cl₂ (200 mL), and the filtrate was dried (MgSO₄) and concentrated in vacuo. The residue was subjected to column chromatography (SiO₂, CH₂Cl₂) to provide the product **10** (0.707 g, 82%) as a colorless oil that solidified upon standing. ¹H NMR (300 MHz, CDCl₃): δ = 0.26 (s, 9H), 1.13 (m, 21H), 2.10 (m, 2H), 4.79 (d, *J* = 5.9 Hz, 2H), 4.81 (d, *J* = 5.9 Hz), 7.54 (s, 2H). ¹³C NMR (75 MHz, CDCl₃): δ = 0.0, 11.4, 18.8, 63.5, 63.6, 98.4, 101.7, 102.2, 104.0, 121.4, 121.8, 131.0, 131.3, 142.2 (two overlapping; i.e., one signal). MS (FAB): *m/z* = 415.3 [M + H⁺]. Anal. Calcd for C₂₄H₃₈O₂Si₂: C, 69.50; H, 9.24. Found: C, 69.16; H, 9.25.

Compound 11. To a solution of the diol **10** (0.667 g, 1.61 mmol) in dry CH₂Cl₂ (45 mL) was added molecular sieves (4 Å, 0.7 g) and Celite (0.65 g). The mixture was stirred for 5 min, whereupon PCC (1.28 g, 5.93 mmol) was added. After stirring for 3.5 h, the mixture was filtered through a short column (SiO₂, CH₂Cl₂), providing the product **11** (0.639 g, 97%) as a yellow analytically pure oil. ¹H NMR (300 MHz, CDCl₃): δ = 0.29 (s, 9H), 1.14 (m, 21H), 8.07 (s, 1H), 8.08 (s, 1H), 10.54 (s, 1H), 10.59 (s, 1H). ¹³C NMR (75 MHz, CDCl₃): δ (ppm) = −0.2, 11.4, 18.8, 98.8, 100.7, 103.0, 105.8, 126.3, 126.6,

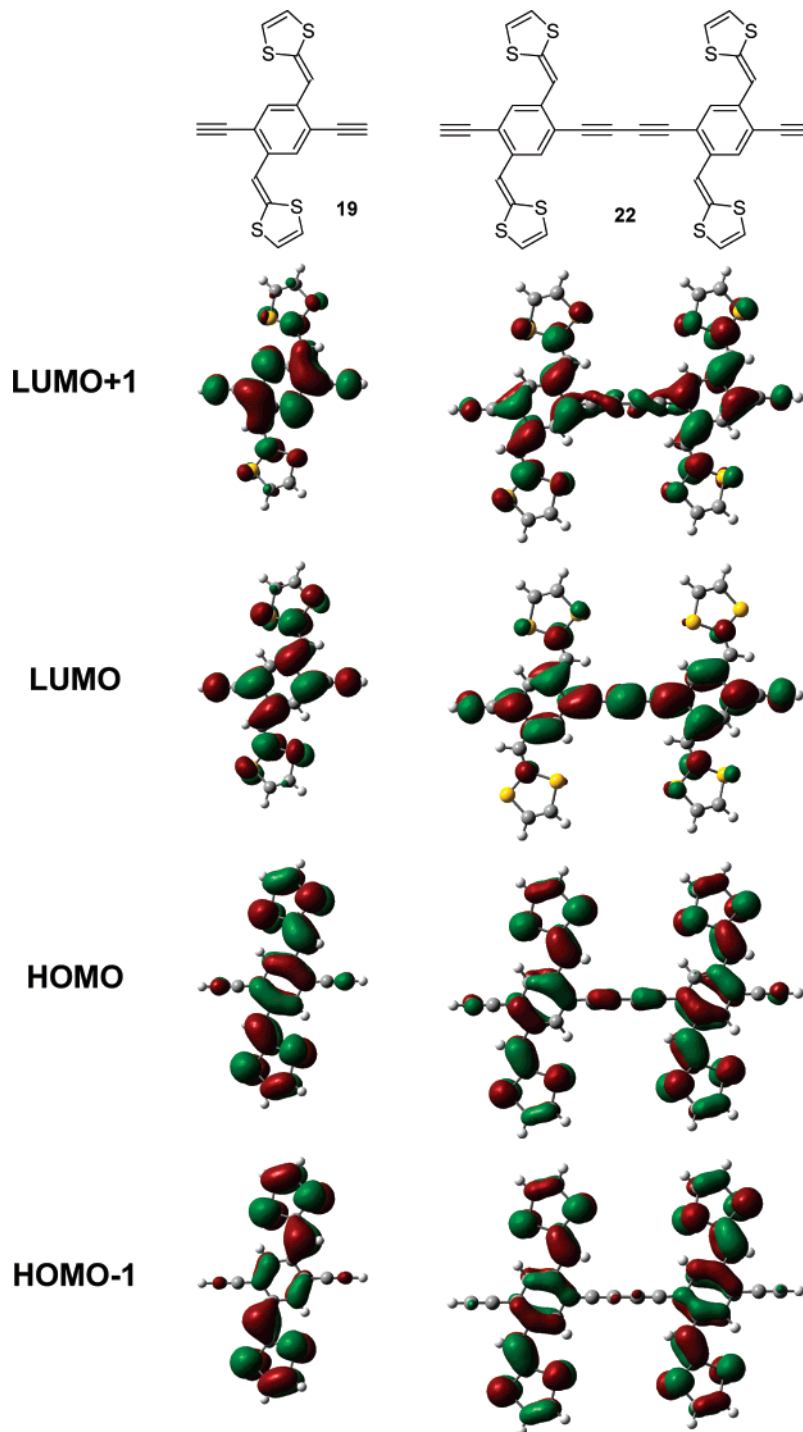


FIGURE 6. Frontier orbitals calculated at B3LYP/6-31G(d) level.

132.6, 132.7, 138.7, 138.8, 190.5, 190.7. MS (FAB): $m/z = 411.3 [M + H^+]$. Anal. Calcd for $C_{24}H_{34}O_2Si_2$: C, 70.19; H, 8.34. Found: C, 70.16; H, 8.46.

Compound 3. Compounds **11** (0.311 g, 0.76 mmol) and **12** (0.974 g, 1.92 mmol) were dissolved in dry MeCN (5 mL) and THF (15 mL), whereupon NEt_3 (0.37 mL, 2.56 mmol) was dropwise added. After stirring for 3 h, the mixture was diluted with CH_2Cl_2 (45 mL), washed with H_2O (3×25 mL), dried ($MgSO_4$), and concentrated in vacuo. Column chromatography (SiO_2 , CH_2Cl_2) gave the product **3** (0.460 g, 81%) as a red solid. Mp 134–137 °C. IR (KBr): $\nu = 3439$ (w), 3013 (w), 2953

(m), 2865 (m), 2149 (w), 1734 (s), 1586 (s), 1470 (w), 1434 (m), 1400 (w), 1258 (s), 1094 (m), 1028 (m), 996 (w), 869 (m), 846 (m), 760 (m), 679 (w) cm^{-1} . 1H NMR (300 MHz, $CDCl_3$): $\delta = 0.29$ (s, 9H), 1.16 (m, 21H), 3.85 (s, 12H), 6.84 (s, 1H), 6.84 (s, 1H), 7.38 (s, 1H), 7.42 (s, 1H). ^{13}C NMR (75 MHz, $CDCl_3$): $\delta = 0.1, 11.5, 18.9, 53.4, 99.3, 102.6, 102.8, 104.7, 112.7, 112.8, 121.5, 122.1, 128.5, 129.3, 129.8, 131.5, 133.3, 133.5, 135.1, 135.2, 159.9, 160.0, 160.2$ (two overlapping; i.e., one signal); Two signals overlapping. MS (FAB): $m/z = 814 [M^+]$. Anal. Calcd for $C_{38}H_{46}O_8S_4Si_2$: C, 55.99; H, 5.69. Found: C, 56.00; H, 5.63.

Compound 4. Method 1: To a solution of compound **3** (0.113 g, 0.138 mmol) in THF (4 mL) and MeOH (15 mL) was added K_2CO_3 (0.027 g, 0.20 mmol). After stirring for 30 min, the mixture was diluted with Et_2O (100 mL), washed with H_2O (50 mL) and brine (50 mL), dried ($MgSO_4$), and concentrated in vacuo. The residue was redissolved in CH_2Cl_2 (15 mL), and then Hay catalyst (10.0 mL) was added [Hay catalyst: $CuCl$ (0.26 g) and TMEDA (0.32 g) in CH_2Cl_2 (10 mL)]. After stirring for 2 h under air, more CH_2Cl_2 (20 mL) was added, and the mixture was stirred under air overnight. Then CH_2Cl_2 (100 mL) was added, and the mixture was washed with H_2O (50 mL) and brine (50 mL). The organic phase was dried ($MgSO_4$) and concentrated in vacuo. Column chromatography (SiO_2 , CH_2Cl_2) gave the product **4** (0.021 g, 19%) as a red solid.

Method 2: The tetraaldehyde **5** (0.050 g, 0.075 mmol) and phosphonium salt **12** (0.188 g, 0.370 mmol) were dissolved in a mixture of dry THF (10 mL) and dry MeCN (3 mL), whereupon NEt_3 (0.072 mL, 0.520 mmol) was added. After stirring for 3 h at rt, the reaction mixture was poured into CH_2Cl_2 (150 mL). The mixture was washed with water (2×50 mL) and brine (50 mL), dried ($MgSO_4$), filtered, and evaporated to dryness under reduced pressure. Column chromatography (SiO_2 , CH_2Cl_2) gave the product **4** as a red solid (0.102 g, 92%). Mp 207–210 °C dec. 1H NMR (300 MHz, $CDCl_3$): δ = 1.16 (m, 42H), 3.86–3.88 ($3 \times$ s, 24H), 6.87 (s, 2H), 6.96 (s, 2H), 7.48 (s, 2H), 7.50 (s, 2H). ^{13}C NMR (75 MHz, $CDCl_3$): δ = 11.5, 18.9, 53.5 ($\times 2$; i.e., two signals), 53.6 (two overlapping; i.e., one signal), 80.5, 82.0, 100.3, 104.6, 112.0, 112.3, 119.8, 123.0, 129.4, 129.5, 129.6, 132.0, 134.1, 134.9, 135.1, 136.1, 159.7 (two overlapping), 160.1, 160.2; two signals overlapping. MS (FAB): m/z = 1481.5 [M^+]. Anal. Calcd. for $C_{70}H_{74}O_{16}S_8Si_2$: C, 56.65; H, 5.03. Found: C, 56.56; H, 4.94.

Compound 13. Compound **9** (0.563 g, 1.13 mmol) and K_2CO_3 (0.138 g, 1.00 mmol) were dissolved in THF (20 mL), whereupon MeOH (10 mL) was added. After stirring for 8 h at rt under an argon atmosphere, the mixture was poured into CH_2Cl_2 (150 mL). The organic phase was washed with water (3×100 mL), brine (75 mL), dried ($MgSO_4$), filtered, and evaporated to dryness under reduced pressure to give the product (0.360 g, 80%) as a yellow solid. Mp 78–79 °C. 1H NMR (300 MHz, $CDCl_3$): δ = 1.15 (m, 21H), 3.50 (s, 1H), 3.92 (s, 3H), 3.96 (s, 3H), 8.08 (s, 1H), 8.10 (s, 1H). ^{13}C NMR (75 MHz, $CDCl_3$): δ = 11.4, 18.8, 52.8, 81.0, 84.7, 100.3, 103.6, 122.0, 123.5, 134.8, 135.3, 136.6, 136.7, 165.4, 165.7. MS (FAB): m/z = 399.1 [$M + H^+$]. Anal. Calcd for $C_{23}H_{30}O_4Si$: C, 69.31; H, 7.59. Found: C, 69.34; H, 7.66.

Compound 14. Compound **13** (0.635 g, 1.49 mmol) was dissolved in CH_2Cl_2 (50 mL). Then Hay catalyst (1.5 mL) was added, and the mixture was vigorously stirred under air for 14 h. The mixture was diluted with CH_2Cl_2 (100 mL), and the organic phase was washed with water (2×100 mL), brine (100 mL), dried ($MgSO_4$), filtered, and evaporated to dryness under reduced pressure to a red foam. Column chromatography (SiO_2 , $EtOAc$ /heptane 1:9) gave the product **14** (0.430 g, 68%) as slightly yellow crystals. Mp 153–55 °C. 1H NMR (300 MHz, $CDCl_3$): δ = 1.15 (m, 42H), 3.93 (s, 6H), 3.99 (s, 6H), 8.13 (s, 2H), 8.15 (s, 2H). ^{13}C NMR (75 MHz, $CDCl_3$): δ = 11.4, 18.8, 52.8, 53.0, 80.9, 81.7, 101.2, 103.7, 121.6, 123.9, 134.9, 135.4, 137.0 ($\times 2$; i.e., two signals), 165.0, 165.5. MS (FAB): m/z = 795.6 [$M + H^+$]. Anal. Calcd for $C_{46}H_{58}O_8Si_2$: C, 69.49; H, 7.35. Found: C, 69.78; H, 7.57.

Compound 15. The tetraester **14** (0.100 g, 0.126 mmol) was dissolved in dry THF (7 mL) and cooled to 0 °C. DIBAL-H (1.40 mL, 1.40 mmol, 1 M in hexane) was added over a period of 5 min. After stirring for 3 h at 0 °C, the reaction mixture was allowed to warm to rt. After stirring for another 24 h, H_2O (2 mL) was added, and the mixture was poured into CH_2Cl_2 (100 mL). The organic phase was washed with 0.08 M HCl (2×50 mL), brine (50 mL), dried ($MgSO_4$), filtered, and evaporated to dryness under reduced pressure to give the product **15** (0.073 g, 85%) as slightly yellow crystals. 1H NMR (300 MHz, $CDCl_3$): δ = 1.13 (m, 42H), 1.94 (t, J = 6.5 Hz, 2H), 2.14 (t, J = 6.5 Hz, 2H), 4.83 (d, J = 6.5 Hz, 4H), 4.86 (d, J = 6.5 Hz, 4H), 7.62 (s, 2H), 7.64 (s, 2H). ^{13}C NMR (75 MHz, $CDCl_3$): δ = 11.5, 18.9, 63.2, 63.5, 79.7, 81.0, 99.6, 103.9, 119.9, 122.8, 131.5, 131.7, 142.5, 143.2. HR-MS (FAB): m/z = 682.3891 [M^+] calcd for $C_{42}H_{58}O_4Si_2$, 682.3874.

Compound 5. The tetraol **15** (0.071 g, 0.104 mmol) was dissolved in dry CH_2Cl_2 (15 mL), whereupon molecular sieves (4 Å), Celite (1 g), and PCC (0.157 g, 0.728 mmol) were added. After stirring for 3 h at rt, the mixture was filtered through a dry column (SiO_2), and the column was washed with additional CH_2Cl_2 (100 mL). The combined organic fractions were evaporated to dryness under reduced pressure to give the product **5** (0.060 g, 86%) as a white solid. 1H NMR (300 MHz, $CDCl_3$): δ = 1.14–1.16 (m, 42H), 8.12 (s, 2H), 8.20 (s, 2H), 10.51 (s, 2H), 10.60 (s, 2H). ^{13}C NMR (75 MHz, $CDCl_3$): δ = 11.4, 18.8, 79.4, 81.7, 100.5, 104.7, 123.5, 127.8, 133.6, 133.8, 138.9, 139.9, 189.4, 190.0. MS (FAB): m/z = 675.3 [M^+]. Anal. Calcd for $C_{42}H_{50}O_4Si_2$: C, 74.73; H, 7.47. Found: C, 74.59; H, 7.73.

Compound 16. The triflate **8** (1.00 g, 2.14 mmol) was dissolved in dry CH_2Cl_2 (6 mL) and cooled to –78 °C. DIBAL-H (1 M in hexane, 9.65 mL, 9.65 mmol) was added over a period of 5 min. After stirring for 45 min at –78 °C, the solution was allowed to warm to rt, and after another 2 h it was poured into CH_2Cl_2 (450 mL). The combined organic phase was washed with 0.08 M HCl (100 mL) and saturated aqueous NH_4Cl (100 mL). The organic phase was dried ($MgSO_4$), filtered, and evaporated to dryness under reduced pressure to give the product **16** as a white solid (0.619 g, 75%). Mp 89–92 °C. 1H NMR (300 MHz, $CDCl_3$): δ = 0.26 (s, 9H), 1.89 (t, J = 6.2 Hz, 1H), 2.10 (t, J = 6.2 Hz, 1H), 4.77 (d, J = 6.2 Hz, 2H), 4.84 (d, J = 6.2 Hz, 2H), 7.42 (s, 1H), 7.70 (s, 1H). ^{13}C NMR (75 MHz, $CDCl_3$): δ = 0.0, 59.3, 62.9, 100.4, 102.2, 119.7, 120.8, 121.5, 132.6, 133.8, 145.4, 146.7. MS (FAB): m/z = 383.2 [M^+]. Anal. Calcd for $C_{14}H_{17}F_3O_5SSi$: C, 43.97; H, 4.48. Found: C, 44.22; H, 4.51.

Compound 17. A mixture of the diol **16** (0.550 g, 1.44 mmol), PCC (1.085 g, 5.03 mmol), Celite (2.0 g), and molecular sieves (4 Å) in dry CH_2Cl_2 (40 mL) was stirred for 3 h at rt. Then the reaction mixture was filtered through a short, dry silica gel column, and the column was washed with additional CH_2Cl_2 (150 mL). Concentration in vacuo gave the product **17** as an oil, which slowly solidified upon standing (0.506 g, 93%). Mp 49–52 °C. 1H NMR (300 MHz, $CDCl_3$): δ = 0.30 (s, 9H), 7.88 (s, 1H), 8.17 (s, 1H), 10.28 (s, 1H), 10.53 (s, 1H). ^{13}C NMR (75 MHz, $CDCl_3$): δ = –0.3, 97.2, 107.1, 120.9, 121.2, 127.2, 131.6, 136.3, 140.7, 148.9, 185.3, 189.2. MS (FAB): m/z = 379.0266 [$M + H^+$] calcd for $C_{14}H_{14}F_3O_5SSi_2$, 379.0283.

Compound 18. The dialdehyde **17** (0.449 g, 1.19 mmol) and phosphonium salt **12** (1.507 g, 2.97 mmol) were dissolved in a

mixture of dry THF (30 mL) and dry MeCN (10 mL). Then NEt₃ (0.578 mL, 4.15 mmol) was added. After stirring for 12 h at rt, the mixture was evaporated to dryness under reduced pressure. The residue was redissolved in CH₂Cl₂ (200 mL) and washed with water (2 × 100 mL) and brine (100 mL), dried (MgSO₄), filtered, and evaporated to dryness under reduced pressure. Column chromatography (SiO₂, CH₂Cl₂) gave the product as a red solid (0.826 g, 89%). Mp 182–186 °C. ¹H NMR (300 MHz, CDCl₃): δ = 1.54 (s, 9H), 3.87–3.88 (2 × s, 12H), 6.43 (s, 1H), 6.88 (s, 1H), 7.24 (s, 1H), 7.52 (s, 1H). MS

(FAB): $m/z = 782.2$ [M⁺]. Anal. Calcd for C₂₈H₂₅F₃O₁₁S₅Si: C, 42.96; H, 3.22. Found: C, 42.92; H, 3.19.

Acknowledgment. The Danish Research Agency is acknowledged for financial support (Grant 2111-04-0018).

Supporting Information Available: General experimental methods; NMR spectra of compounds **3–5**, **8–11**, **13–18**; tables of atom coordinates and absolute energies of **19–22** and benzene. This material is available free of charge via the Internet at <http://pubs.acs.org>.

JO702735D